Mining Multi-Label Samples from Single Positive Labels

Anonymous Author(s)
Affiliation
Address
email

Abstract

Conditional generative adversarial networks (cGANs) have shown superior results in class-conditional generation tasks. In order to simultaneously control multiple conditions, cGANs require multi-label training datasets, where multiple labels can be assigned to each data instance. Nevertheless, the tremendous annotation cost limits the accessibility of multi-label datasets in the real-world scenarios. Hence, we explore the practical setting called *single positive setting*, where each data instance is annotated by only one positive label with no explicit negative labels. To generate multi-label data in the single positive setting, we propose a novel sampling approach called single-to-multi-label (S2M) sampling, based on the Markov chain Monte Carlo method. As a widely applicable "add-on" method, our proposed S2M sampling enables existing unconditional and conditional GANs to draw high-quality multi-label data with a minimal annotation cost. Extensive experiments on real image datasets verify the effectiveness and correctness of our method, even when compared to a model trained with fully annotated datasets.

1 Introduction

Since proposed by Goodfellow *et al.* [1], generative adversarial networks (GANs) gained much attention due to its realistic output in a wide range of applications, *e.g.*, image synthesis [2, 3, 4], image translation [5, 6, 7, 8], and data augmentation [9, 10]. As an advanced task, generating images from a given condition has been achieved by conditional GANs (cGANs) and its variants [11, 12]. To reflect the nature of real data where each data instance can belong to multiple classes, multi-label datasets have been introduced in the applications of cGANs [8, 13]. In a multi-label dataset, each data instance can be specified with multiple attributes. For example, in a multi-label facial image dataset, each image is labeled for entire classes such as *Black-hair*, *Smile*, and *Male*. The label for each class is given as a binary value and indicates the presence or absence of the corresponding attribute. Despite its usefulness, as claimed in earlier studies [14, 15, 16], access to multi-label datasets is severely limited in practice due to the difficulty of annotating all attributes. Under these circumstances, weakly annotated dataset is used as an alternative for cGANs to reduce the annotation cost.

In this paper, we introduce the *single positive setting* [16], originally proposed for classification tasks, to conditional generation. Each data instance has a label indicating only the presence of one attribute (*i.e.*, a single positive label) in this setting, and the presence of the rest of the attributes remains unknown. For instance, in a facial image dataset, all attributes are fully specified in a multi-label setting (*e.g.*, *Smiling black-haired man*) whereas only one attribute is specified in the single positive setting (*e.g.*, *Black-hair*). The single positive setting allows us not only to reduce the annotation cost, but also to model the intrinsic relationships among classes.

To generate multi-label data using only single positive labels, we consider two types of combinatorial classes from two classes A and B that each corresponds to a single positive label: (1) *overlapping*

Submitted to 36th Conference on Neural Information Processing Systems (NeurIPS 2022). Do not distribute.

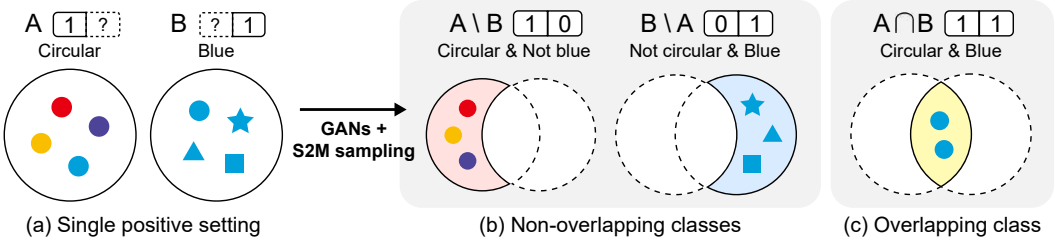

Figure 1: Illustration of joint classes where two attributes (circular, blue) are given. (a) Only one of the attributes is specified in the single positive setting. From classes A and B, our S2M sampling can draw samples from three joint classes: (b) two non-overlapping classes ($A \setminus B$ and $B \setminus A$) and (c) one overlapping class ($A \cap B$).

class, where the data instances belong to both classes ($A \cap B$), and (2) *non-overlapping class*, where the data instances belong to only one of the classes ($A \setminus B$ or $B \setminus A$). Figure 1 shows an example of overlapping class and non-overlapping classes when two types of single positive label are given. By extending this concept, we can consider combinatorial classes, where data instances belong to certain classes but not to the rest. We denote these classes as *joint classes*. By accessing a joint class, we can generate multi-label samples using only single positive labels. Ideally, we can represent all possible label combinations with at least one positive label.

Several attempts have been made to consider such a joint class in generation tasks. Specially designed generative models such as GenPU [17] and RumiGAN [18] were proposed to generate samples from one class while excluding another class. However, these studies dealt with only two classes and did not consider the overlapping class. Recently, Kaneko *et al.* [19] proposed CP-GAN to capture between-class relationships in conditional generation. To generate images belonging to n classes, they equally assign $1/n$ as the class posterior for each selected class. This means that CP-GAN generates images that have an equal probability of being classified as each class. However, due to the fact that an image in the real world that belongs to multiple classes does not have equal class posteriors, leading to the loss of sample diversity. In consequence, we focus on a sampling approach to precisely draw samples from complex distributions that are difficult to directly sample. In recent studies of GANs, sampling approaches [20, 21] employed the rejection sampling or Markov chain Monte Carlo method to obtain realistic data. They adopt the sampling process as the post-processing method of GANs and filter generated images using the pretrained classifiers.

In line with these studies, we propose a novel sampling framework called *single-to-multi-label (S2M) sampling* to correctly generate data from both overlapping and non-overlapping classes. We newly propose a tractable formulation to estimate the conditional density of joint classes. Concretely, we employ several classification networks to estimate the target conditional density and apply Markov chain Monte Carlo method upon pretrained unconditional and conditional GANs. In Figure 2, we depict the conceptual difference against the existing approaches (1st row) and provide the empirical results on 1D Gaussian example (2nd row). Due to the fact that S2M sampling performs at the inference time of generation, it fully preserves the image quality and eliminates the need for changing the objective functions and architectures. We validate the effectiveness of our method compared to the existing models on diverse datasets such as MNIST, CIFAR-10 and CelebA. To the best of our knowledge, our approach is the first sampling framework that generates multi-label data from single positive labels. Our contributions can be summarized as follows:

- We introduce the single positive setting in conditional generation task and provide the theoretical framework for estimating conditional densities of joint classes.
- We propose a novel sampling framework based on Markov chain Monte Carlo method for generating multi-label data from single positive labels.
- Through vast experiments, we show that our S2M sampling correctly draws multi-label data while fully preserving the quality of generated images.

2 Related Work

Conditional GANs. The aim of conditional GANs (cGANs) [11] is to model complex distributions and to control data generation by reflecting the label input. Various studies of cGANs have made significant advances in class-conditional image generation by introducing the auxiliary classifier [12,

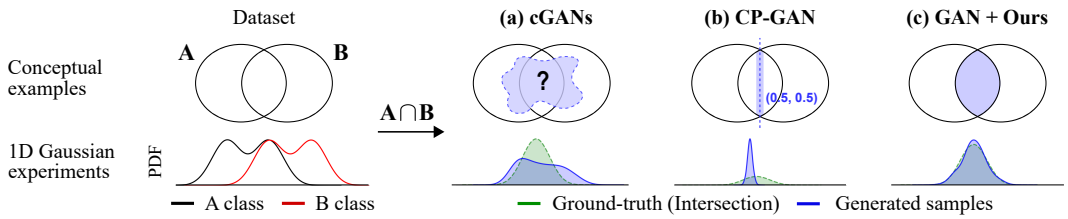

Figure 2: We compare cGANs, CP-GAN and our method in a class-overlapping case. 1D Gaussian examples consists of two classes of one-dimensional Gaussian mixtures with one common mode, and each method attempts to generate samples in the overlapping region. For cGANs and CP-GAN, we provide an equal value of 0.5 as labels for two classes. (a) It is not clear how cGANs obtain samples of the class. (b) CP-GAN draws samples from the narrow region. (c) GAN with S2M sampling draws samples accurately without sacrificing diversity.

22], modifying the architecture [23, 2], and applying metric learning [24]. In a weakly-supervised setting, GenPU [17] and RumiLSGAN [18] specify only two classes and draw samples that belong to one class but not the other. CP-GAN [19] learns to draw samples conditioned on the probability output of the classifier. Given that this model tends to draw samples on a limited region of the data space, it is challenging to ensure the variety of samples as shown in Figure 2. In contrast, we propose a sampling method that draws multi-label samples without sacrificing diversity.

Sampling in GANs. Sampling methods are used to improve the sample quality in GANs. Discriminator rejection sampling [20] uses the scheme of rejection sampling and takes samples close to real data by estimating the density ratio with the discriminator. In addition, Metropolis-Hastings GAN [21] adopts Markov chain Monte Carlo (MCMC) method and calibrates the discriminator to improve the sample quality in a high-dimensional data space. Discriminator driven latent sampling [25] uses the MCMC method in the latent space of GANs to draw realistic samples efficiently. GOLD estimator [26] uses a sampling algorithm to improve the quality of images for class-conditional generation. While previous studies focus on improving the sample quality, our S2M sampling aims to draw multi-label samples while also improving the quality.

3 Methods

3.1 Problem Setting

Let $x \in X$ be a data point as a random variable and let $y_{1:n} \in \{0,1\}^n$ denote its corresponding multi-labels as binary random variables. Here, for every k, $y_k = 1$ indicates that x is contained in the k-th class while $y_k = 0$ indicates that x is not. We consider two index sets, an intersection index set I and a difference index set J, so that the pair (I, J) can be used as an index to indicate the class, where data points contained in all classes indicated by I but excluded from all classes indicated by J. Let $\mathcal{I}$ be a collection of all possible pairs of I and J, defined as

$$\mathcal{I} = \{(I, J) \in \mathcal{P}(N) \times \mathcal{P}(N) : I \neq \emptyset, I \cap J = \emptyset\}, \tag{1}$$

where $N = \{1, 2, ..., n\}$ is a finite index set of all classes and $\mathcal{P}(N)$ is the power set of N. That is, the intersection index set indicates at least one class and is distinct from the difference index set. Especially for $I \cup J = N$, the class indicated by (I, J) is called the *joint class*.

Let $p(x, y_1, y_2, ..., y_n)$ be the joint probability density function, and let $p_{data}(x, c)$ be the joint density of an observed data point $x \in X$ and a class label $c \in N$ such that $p_{data}(x|c) = p(x|y_c = 1)$. Given the class priors $p_{data}(c), \pi_c := p(y_c = 1)$ and samples drawn from the class-conditional density $p_{data}(x|c)$ for each $c = 1, 2, ..., n$, our goal is to draw samples from the conditional density

$$p_{(I,J)}(x) := p(x|\forall i \in I, \forall j \in J, y_i = 1, y_j = 0), \tag{2}$$

for $(I, J) \in \mathcal{I}$, and $\pi_{(I,J)} := p(\forall i \in I, \forall j \in J, y_i = 1, y_j = 0) > 0$. In this work, we propose to impose a mild constraint which will allow our sampling algorithm to derive the target density.

Assumption 1. *For every $i, j \in N$ such that $i \neq j$, if $p(y_i = 1, y_j = 0) > 0$ and $p(y_j = 1, y_i = 0) > 0$, then* $\operatorname{supp} p(x|y_i = 1, y_j = 0) \cap \operatorname{supp} p(x|y_j = 1, y_i = 0) = \emptyset$.

The Assumption 1 states that no data points are likely to be assigned two mutually exclusive labels, which can be naturally assumed in many practical situations. Figure 3 illustrates our problem setting.

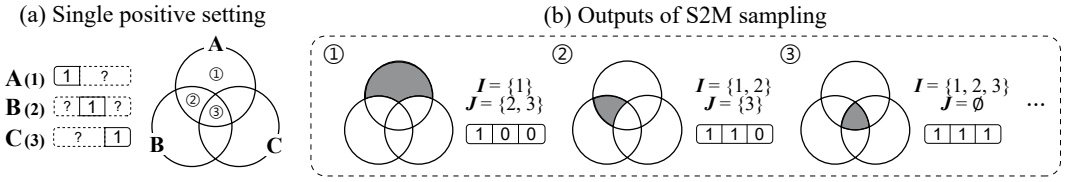

Figure 3: (a) A dataset with single positive labels is given. (b) S2M sampling can draw samples as multi-label data with two index sets of intersection (I) and difference (J).

3.2 Mining Multi-Label Data with S2M Sampling

A natural question may arise as to whether the supervision given to us is sufficient to obtain multi-label samples. To gain insight into this, we derive a useful theorem which provides an alternative formulation for the target density (2).

Theorem 1. *Let $\{f_{(I,J)} : X \to [0,\infty)\}_{(I,J)\in\mathcal{I}}$ be an indexed family of non-negative measurable functions on X, and let $f_k := f_{(\{k\},\emptyset)}$. Then, the following conditions hold:*

(a) $\forall (I,J) \in \mathcal{I}, f_{(I,J)} = \sum_{S:I\subseteq S, J\subseteq N\setminus S} f_{(S,N\setminus S)}$

(b) $\forall i,j \in N$ *s.t.* $i \neq j, \operatorname{supp} f_{(\{i\},\{j\})} \cap \operatorname{supp} f_{(\{j\},\{i\})} = \emptyset$

if and only if, for every $(I,J) \in \mathcal{I}$,

$$f_{(I,J)} = \begin{cases} (\min_{i\in I} f_i - \max_{j\in J} f_j)^+ & \text{if } J \neq \emptyset \\ \min_{i\in I} f_i & \text{otherwise} \end{cases}, \tag{3}$$

where $(\cdot)^+$ represents the positive part.

Proof. Please see Appendix. □

Let $f_{(I,J)}(x) = p(x, \forall i \in I, \forall j \in J, y_i = 1, y_j = 0)$ for every $(I,J) \in \mathcal{I}$. Then, both (a) and (b) in Theorem 1 hold by the Assumption 1. According to the Theorem 1, if $\pi_{(I,J)} > 0$,

$$p_{(I,J)}(x) = \pi_{(I,J)}^{-1}(\min\{\pi_i p(x|y_i = 1) : i \in I\} - \max\{\pi_j p(x|y_j = 1) : j \in J\} \cup \{0\})^+. \tag{4}$$

The alternative formula (4) shows that the density of joint class can be derived from the class-conditional densities of single positive labels. Despite their clear relationship, training a generator that can model the density $p_{(I,J)}$ is non-trivial problem since the formula consists of several implicitly defined conditional densities, class priors, and variable sets. To address this issue, we propose to apply sampling approaches upon existing GANs. Interestingly, our sampling framework called S2M sampling allows not only to draw samples from the target density, but also to modify I, J, and class priors at inference time. The rest of this section introduces the main approaches of our S2M sampling.

Density Ratio Estimation. We utilize several classification networks to compute implicitly defined density ratios. For simplicity, we denote G as a pretrained generator for both unconditional and conditional GANs. G produces data x by taking a latent z and a class label c for class-conditional generation and only z for unconditional generation. We consider three classifiers D_v, D_r, and D_f which are obtained by minimizing $\mathcal{L}_v, \mathcal{L}_r$, and $\mathcal{L}_f$, respectively, *i.e.*,

$$\begin{aligned} \mathcal{L}_v &= -\mathbb{E}_{(x,c)\sim p_{data}(x,c)}[\log D_v(x)] - \mathbb{E}_{x\sim p_G(x)}[\log(1 - D_v(x))], \\ \mathcal{L}_r &= -\mathbb{E}_{(x,c)\sim p_{data}(x,c)}[\log D_r(c|x)],\ \mathcal{L}_f = -\mathbb{E}_{(x,c)\sim p_G(x,c)}[\log D_f(c|x)], \end{aligned} \tag{5}$$

where p_G is the distribution of generated samples by G. The optimal classifiers trained by these losses D_v^*, D_r^*, and D_f^* satisfy the following equations: $D_v^*(x) = p_{data}(x)/(p_{data}(x)+p_G(x))$, $D_r^*(c|x) = p(x|y_c = 1)p_{data}(c)/p_{data}(x)$, $D_f^*(c|x) = p_G(x|c)p_G(c)/p_G(x)$. From D_v^*, D_r^*, and D_f^*, we can access the density ratios $p_{data}(x)/p_G(x)$, $p(x|y_c = 1)/p_{data}(x)$, and $p_G(x|c)/p_G(x)$ which will be used to compute the acceptance probability of the MCMC method.

S2M Sampling for Unconditional GANs. We apply Metropolis-Hastings (MH) independence sampling [27, 21] to draw samples from the complex target distribution p_t. MH algorithm uses a Markov process where each transition from a current state x_k to next state x_{k+1} is made by accept-reject step. At each step of MH independent sampling, we sample a new proposal x' from a proposal distribution $q(x'|x) = q(x')$ and then accept it with probability $\alpha(x', x)$ which is given

by $\alpha(x', x) = \min\left(1, \frac{p_t(x')q(x)}{p_t(x)q(x')}\right)$. We set $x_{k+1} = x'$ if x' is accepted, $x_{k+1} = x_k$ otherwise. Then, the chain of samples $x_{1:K}$ converges to the unique stationary distribution p_t as $K \to \infty$.

Given a generator G where the support of p_G contains that of $p_{(I,J)}$. To draw samples from $p_{(I,J)}$, we let $p_t = p_{(I,J)}$ and take multiple samples from G as independent proposals, i.e. $q(x'|x) = p_G(x')$. Then, the desired acceptance probability $\alpha(x', x)$ can be calculated using D_v^* and D_r^*:

$$r_{(I,J)}(x) \coloneqq \left(\min\left\{\frac{\pi_i}{p_{data}(i)} D_r^*(i|x) : i \in I\right\} - \max\left\{\frac{\pi_j}{p_{data}(j)} D_r^*(j|x) : j \in J\right\} \cup \{0\}\right)^+,$$
$$\alpha(x', x) = \min\left(1, \frac{p_{(I,J)}(x')/p_G(x')}{p_{(I,J)}(x)/p_G(x)}\right) = \min\left(1, \frac{r_{(I,J)}(x')(D_v^*(x)^{-1} - 1)}{r_{(I,J)}(x)(D_v^*(x')^{-1} - 1)}\right). \tag{6}$$

Different from Turner *et al.* [21], the term $r_{(I,J)}(x')/r_{(I,J)}(x)$ is added to the acceptance probability formula to draw multi-label samples. To obtain uncorrelated samples, we take a sample after a fixed number of iterations for each chain. We note that the sampling approach allows one to control the parameters I, J, and $\gamma_k \coloneqq \pi_k/p_{data}(k)$ without any additional training of the model. A summary of our S2M sampling algorithm is provided in Appendix.

S2M Sampling for Conditional GANs. cGANs can provide a proposal distribution close to the target distribution $p_{(I,J)}$, which greatly increases the sample efficiency of the MCMC method. Let c be a class label such that the support of class-conditional density $p_G(\cdot|c)$ contains that of $p_{(I,J)}$. At each step of the MH algorithm, the proposal $x' \sim q(x'|x) = p_G(x'|c)$ is accepted with a probability $\alpha_c(x', x)$. The desired $\alpha_c(x', x)$ can be calculated as

$$\alpha_c(x', x) = \min\left(1, \frac{p_{(I,J)}(x')/p_G(x'|c)}{p_{(I,J)}(x)/p_G(x|c)}\right) = \min\left(1, \frac{r_{(I,J)}(x')D_f^*(c|x)(D_v^*(x)^{-1} - 1)}{r_{(I,J)}(x)D_f^*(c|x')(D_v^*(x')^{-1} - 1)}\right). \tag{7}$$

That is, the sampling method can be adopted to cGANs by additionally computing $D_f^*(c|x)/D_f^*(c|x')$.

Latent Adaptation in S2M Sampling. While our S2M sampling allows us to draw multi-label samples, the algorithm rejects certain samples through the sampling procedure if the target distribution $p_{(I,J)}$ is significantly different from the generator distribution. Specifically, independent MH algorithm takes time inversely proportional to the probability of a generated sample belonging to the target class (See Appendix). To alleviate this issue, we propose a technique to improve the sample efficiency from past sampling attempts. We initially draw a certain number of pilot target class samples $x_{1:m}$ using S2M sampling, and then obtain the corresponding target latent samples $t_{1:m}$; $x_k = G(t_k)$. Since the latent samples are nearly restricted to the latent prior of GANs (*e.g.*, Gaussian distribution), we can roughly estimate the distribution $\tilde{p}_z$ of the target latent by fitting a simple probabilistic model using $t_{1:m}$. Let $\tilde{p}_G$ be the newly obtained generator distribution induced by G, *i.e.*, $G(z) = x \sim \tilde{p}_G(x)$ for $z \sim \tilde{p}_z(z)$. We can further improve the sample efficiency by using $\tilde{p}_G$ as the proposal distribution in the MH algorithm since $\tilde{p}_G$ is much close to the target distribution. To run the MH algorithm without retraining the classifiers, we approximate $p_G(G(z))/\tilde{p}_G(G(z)) \approx C \cdot p_z(z)/\tilde{p}_z(z)$[1] for some constant C. Then, at each step of the MH algorithm, the proposal $x' \sim q(x'|x) = \tilde{p}_G(x')$ is accepted with a probability $\tilde{\alpha}(x', x)$ which can be calculated as

$$\tilde{\alpha}(x', x) = \min\left(1, \frac{p_{(I,J)}(x')/\tilde{p}_G(x')}{p_{(I,J)}(x)/\tilde{p}_G(x)}\right) \approx \min\left(1, \frac{r_{(I,J)}(x')(D_v^*(x)^{-1} - 1)p_z(z')/\tilde{p}_z(z')}{r_{(I,J)}(x)(D_v^*(x')^{-1} - 1)p_z(z)/\tilde{p}_z(z)}\right), \tag{8}$$

where $x' = G(z')$ and $x = G(z)$. Here, we can explicitly compute the density ratio between p_z and $\tilde{p}_z$ by letting $\tilde{p}_z$ be a known probability density function such as Gaussian mixture. In practice, if the target class samples rarely appear in generated samples, one can consider applying latent adaptation repeatedly. For instance, to draw *Black-haired man* samples, we can first search the latent space of *Man* by using latent adaptation, and then perform it in that space again to search the space of *Black-haired man*. In terms of time complexity, this is performed more efficiently than searching the space of *Black-haired man* at once. Detailed discussion about the time complexity and the description of latent adaptation are provided in Appendix.

[1]The equation is derived in the previous latent sampling approaches by the reverse lemma of rejection sampling [25] or the change-of-variables formula [28].

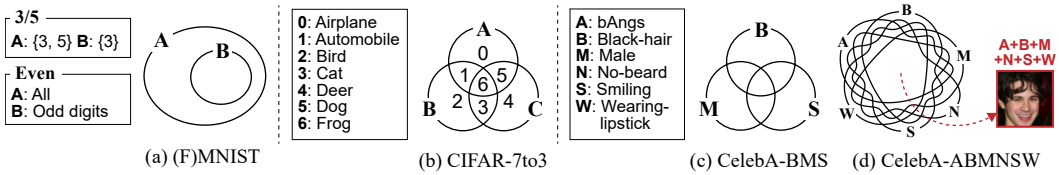

(a) (F)MNIST (b) CIFAR-7to3 (c) CelebA-BMS (d) CelebA-ABMNSW

Figure 4: Experimental settings for (F)MNIST, CIFAR-7to3, CelebA-BMS, and CelebA-ABMNSW.

Practical Considerations. We employ three classifiers D_v, D_r, and D_f, to compute the acceptance probability used in MCMC method. For better training efficiency of the classifiers, we use shared layers, except for the last linear layer. Since the classifiers are not optimal in practice, we scale the temperature of classifiers [29] and adjust γ_k to calibrate the sampling algorithm. We provide the detailed settings and the ablation study in Appendix.

4 Experiments

In this section, we validate that our S2M sampling properly draw samples within the joint classes. Specifically, we mainly consider two cases in the single positive setting: (i) one class is entirely contained in another class, (ii) multiple classes are partially overlapped with each other. In the former setting, we verify that our S2M sampling can completely filter out samples of a smaller class, and compare our method to the existing models including GenPU [17] and RumiLSGAN [18] on MNIST and Fashion-MNIST (FMNIST). In the latter setting, we assess all possible joint classes with our S2M sampling. Subsequently, we evaluate how accurately our S2M sampling draws samples in these classes compared to CP-GAN [19] and the models trained with fully annotated multi-label dataset.

To verify whether a method can accurately generate samples for each joint class, we evaluate *accuracy* which indicates how many generated images are assigned to the target joint classes by a classifier trained with fully annotated data (*i.e.*, multi-label data). Since accuracy itself cannot fully evaluate the distance between the distribution of generated samples and that of real samples, we additionally introduce various metrics to evaluate fidelity (*i.e.*, how realistic the generated samples are) and diversity of generated images: (i) *Inception Score* (IS) [30], (ii) *Fréchet Inception Distance* (FID) [31], (iii) *improved precision and recall* [32], and (iv) *density and coverage* [33].

FID and IS are metrics to evaluate the fidelity and diversity of generated samples using the features of the pretrained Inception-V3 network [34]. A lower FID and a higher IS indicate higher fidelity and diversity of generated samples. Precision and density measure the ratio of generated samples that falls within the manifold of real samples, so that they evaluate the fidelity of generated samples. On the contrary, recall and coverage measure the ratio of real samples that falls within the manifold of generated samples, and thus it evaluates the diversity of generated samples. That is, a higher value of these metrics indicates that the generated samples have a distribution similar to the real one.

Since several metrics for fidelity and diversity are not applicable for non-ImageNet-like images (*e.g.*, MNIST and FMNIST), we instead use FID score computed from activations of LeNet5 [35] and denote this FID†. We use the test set as a reference dataset for evaluating FID. All results are averaged over three independent trials, and the standard deviation is denoted by subscripts. Detailed experimental settings, such as architectures and hyperparameters, are provided in Appendix.

4.1 Sampling for Classes with Inclusion

Experimental Settings. We consider a special case of our problem setting, where one class is entirely contained in another class ($B \subset A$) as shown in Figure 4 (a). This setting is similar to the positive-unlabeled setting [36, 37] where the positive data is included in the unlabeled data. Under this constraint, GenPU [17], RumiLSGAN [18], and CP-GAN [19] can be used to generate samples from the non-overlapping class ($A \setminus B$). Along with these models, we attempt to draw samples from the non-overlapping class by adopting our S2M sampling to unconditional WGAN-GP [38]. These experiments are conducted in three settings (See Figure 4): (i) **MNIST-3/5** (A={3, 5}, B={3}), (ii) **MNIST-Even** (A={0, 1, 2, 3, 4, 5, 6, 7, 8, 9}, B={1, 3, 5, 7, 9}), and (iii) **FMNIST-Even** (A=$\{0_{\text{T-shirt/Top}}, 1_{\text{Trouser}}, 2_{\text{Pullover}}, 3_{\text{Dress}}, 4_{\text{Coat}}, 5_{\text{Sandal}}, 6_{\text{Shirt}}, 7_{\text{Sneaker}}, 8_{\text{Bag}}, 9_{\text{Ankle boot}}\}$, B=$\{1, 3, 5, 7, 9\}$). For S2M sampling, we obtain samples at 100 MCMC iterations.

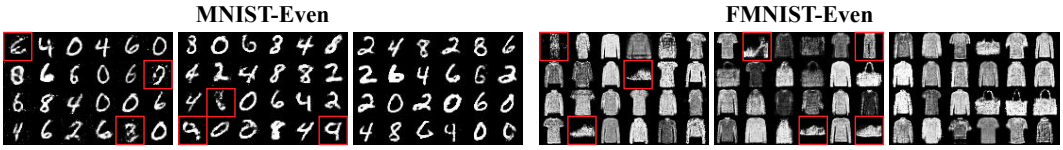

Figure 5: Qualitative results on MNIST-Even and FMNIST-Even.

Quantitative Results. Table 1 shows the results of our S2M sampling and the baselines for the non-overlapping classes. The performance of GenPU is reported only for MNIST-3/5 due to its mode collapse issue [39, 40]. In the results, our S2M sampling adopted to unconditional GAN shows promising results in terms of both accuracy and FID†. In fact, our results prove superior to the existing methods specially designed for generating non-overlapping data such as GenPU and RumiLSGAN. Notably, our S2M sampling improves the accuracy by 8.5% and 6.8% while decreasing FID† compared to the second-best models on MNIST-Even and FMNIST-Even, respectively. This indicates that our S2M sampling accurately samples the images of the non-overlapping classes without being biased to a specific mode.

Table 1: Results for different models on MNIST and FMNIST.

Method	MNIST-3/5		MNIST-Even		FMNIST-Even	
	Acc. (%) (↑)	FID† (↓)	Acc. (%) (↑)	FID† (↓)	Acc. (%) (↑)	FID† (↓)
GenPU [17]	99.33±0.56	1.93±1.10	-	-	-	-
RumiLSGAN [18]	77.06±1.54	13.20±1.19	86.11±4.83	3.44±1.39	91.07±0.88	3.23±2.48
CP-GAN [19]	66.89±1.46	19.50±0.90	87.87±0.40	2.23±0.08	81.21±0.67	6.14±0.56
GAN + Ours	**99.52±0.34**	**0.88±0.21**	**96.37±0.25**	**0.86±0.24**	**97.87±0.66**	**2.48±0.29**

Qualitative Results. Figure 5 shows the qualitative results of RumiLSGAN, CPGAN and our method adopted to WGAN-GP. As indicated by red boxes, RumiLSGAN and CP-GAN fail to completely eliminate the samples of the smaller class (*e.g.*, odd digits for MNIST-Even or *Sneaker* for FMNIST-Even). On the other hand, our S2M sampling correctly draw samples for the target classes.

4.2 Sampling for Multiple Classes

Experimental Settings. We consider a general case of single positive setting where multiple classes can be overlapping as shown in Figure 4 (b-d). Given n classes, at most $2^n - 1$ joint classes can be obtained. In this setting, we attempt to get samples of these joint classes using only single positive labels. We consider cGANs with projection discriminator (cGAN-PD) [23], AC-GAN [12], and CP-GAN [19] as the baseline generative models.

Since the traditional conditional GANs such as cGAN-PD and AC-GAN do not originally designed for generating joint classes, we naively introduce those models in our setting with the slight modification. Concretely, as a method to generate images belonging to n classes, we provide $1/n$ as the conditional value for each class, following Kaneko *et al.* [19]. In our experiments, we expect these models to serve a lower bound performance of our results and indicate their results by asterisks (*). In contrast, conditional GANs trained on a fully annotated dataset where all joint classes are specified as strong baselines in our settings. We train cGAN-PD and AC-GAN in this setting, and denote them as *oracle models*. In the experiments, our S2M sampling is adopted on unconditional GAN and cGAN-PD. When adopting our S2M sampling to cGAN-PD, we use a class containing the target joint class as the conditional value of cGAN-PD. We use BigGAN [2] as the backbone architecture for all generative models, and only single positive labels are used except for the oracle models.

To demonstrate the effectiveness of our S2M sampling, we use three real-world image datasets: (i) **CIFAR-7to3** that has three classes, each of which contains four original classes of CIFAR-10, (ii) **CelebA-BMS** that consists of human face images, each of which is labeled for one of three attributes (*Black-hair*, *Male*, and *Smiling*), and (iii) **CelebA-ABMNSW** that consists of human face images, each of which is labeled for one of six attributes (*bAngs*, *Black-hair*, *Male*, *No-beard*, *Smiling*, and *Wearing-lipstick*). As depicted in Figure 4 (b-d), these datasets can have up to $2^3 - 1$ or $2^6 - 1$ joint classes. For S2M sampling, samples are obtained at 200 MCMC iterations for CIFAR-7to3 and CelebA-BMS, and obtained at 1000 MCMC iterations for CelebA-ABMNSW.

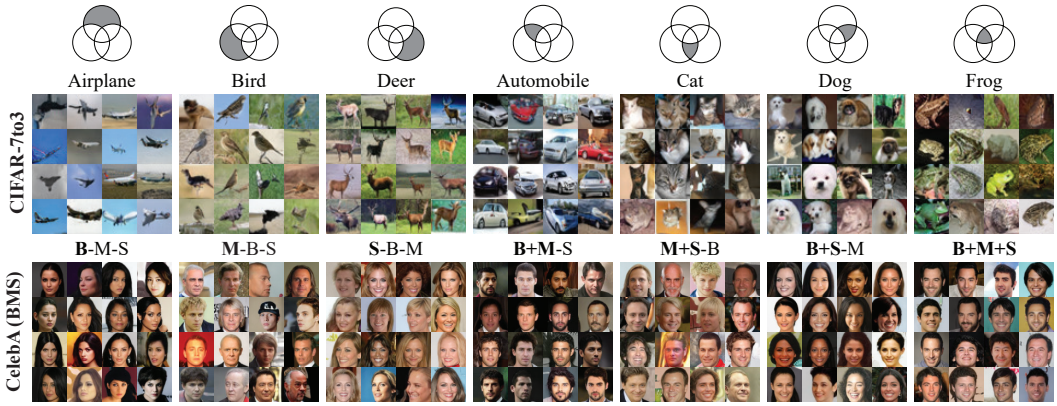

Figure 6: Results of our S2M sampling with cGAN-PD on CIFAR-7to3 and CelebA-BMS. The first row depicts the target joint class.

Table 2: Accuracy (%), FID, IS, precision (P), recall (R), density (D), and coverage (C) for different models on real-world datasets.

	Model	Acc. (↑)	FID (↓)	IS (↑)	P (↑)	R (↑)	D (↑)	C (↑)
CIFAR-7to3	cGAN-PD (Oracle) [23]	87.60±0.15	16.55±0.69	8.39±0.18	0.73±0.01	0.65±0.01	0.89±0.05	0.85±0.02
	AC-GAN (Oracle) [12]	94.14±0.39	16.14±0.43	8.44±0.03	0.74±0.00	0.63±0.00	0.89±0.02	0.84±0.00
	cGAN-PD* [23]	27.19±0.53	21.12±0.62	7.94±0.02	0.71±0.01	0.66±0.00	0.81±0.03	0.78±0.01
	AC-GAN* [12]	31.06±1.17	26.42±0.82	7.31±0.10	0.69±0.01	0.66±0.01	0.71±0.01	0.70±0.01
	CP-GAN [19]	42.62±0.54	27.88±2.00	7.42±0.06	0.71±0.00	0.66±0.00	0.76±0.00	0.71±0.02
	GAN + Ours	77.65±1.22	14.42±0.55	8.71±0.16	0.72±0.00	**0.67±0.00**	0.92±0.02	0.87±0.01
	cGAN-PD + Ours	**80.62±2.08**	**14.14±0.34**	**9.06±0.18**	**0.75±0.01**	0.66±0.01	**1.09±0.12**	**0.90±0.01**
CelebA-BMS	cGAN-PD (Oracle) [23]	78.35±1.99	10.38±0.55	2.45±0.07	0.79±0.03	0.48±0.02	1.12±0.18	0.86±0.02
	AC-GAN (Oracle) [12]	91.57±0.43	10.41±1.52	2.40±0.03	0.79±0.02	0.49±0.04	1.18±0.12	0.86±0.03
	cGAN-PD* [23]	39.84±0.70	10.97±1.56	2.32±0.06	0.79±0.01	0.48±0.04	1.19±0.05	0.86±0.02
	AC-GAN* [12]	52.01±1.81	12.39±1.02	2.32±0.10	0.79±0.02	**0.49±0.01**	1.17±0.09	0.85±0.02
	CP-GAN [19]	87.36±2.05	13.38±1.36	2.43±0.09	0.78±0.01	0.45±0.02	1.08±0.04	0.82±0.02
	GAN + Ours	85.22±4.27	**10.50±0.97**	**2.51±0.08**	0.83±0.02	0.48±0.03	1.36±0.08	**0.89±0.02**
	cGAN-PD + Ours	**90.44±1.05**	10.63±0.29	2.46±0.06	**0.84±0.00**	0.48±0.02	**1.40±0.02**	0.88±0.01
CelebA-ABMNSW	cGAN-PD (Oracle) [23]	69.61±2.91	13.54±2.54	2.44±0.11	0.79±0.02	0.42±0.04	1.15±0.10	0.84±0.02
	AC-GAN (Oracle) [12]	91.37±1.14	13.46±1.29	2.30±0.05	0.80±0.02	0.36±0.01	1.17±0.09	0.82±0.01
	cGAN-PD* [23]	15.28±0.08	11.09±0.67	2.32±0.03	0.80±0.01	**0.47±0.03**	1.19±0.07	0.85±0.02
	AC-GAN* [12]	23.97±0.64	11.92±2.06	2.44±0.06	0.77±0.04	0.45±0.02	1.11±0.13	0.82±0.04
	CP-GAN [19]	79.09±1.14	14.97±4.18	2.45±0.04	0.74±0.03	0.46±0.03	0.95±0.08	0.77±0.06
	GAN + Ours	70.04±2.97	**9.77±0.22**	**2.62±0.05**	0.81±0.01	**0.47±0.01**	1.28±0.04	0.87±0.01
	cGAN-PD + Ours	**79.74±0.78**	10.30±0.48	2.45±0.06	**0.85±0.01**	**0.47±0.02**	**1.45±0.06**	**0.88±0.00**

Quantitative Results. Table 2 summarizes the quantitative results of joint class generation on CIFAR-7to3, CelebA-BMS, and CelebA-ABMNSW. As expected, we can observe that cGAN-PD* and AC-GAN* cannot accurately generate samples from joint classes, which is consistent with the findings of Kaneko *et al.* [19]. Although CP-GAN shows reasonable accuracy for all experiments, it suffers from generating diverse samples. As discussed in Section 1, the high FID and low coverage support that CP-GAN tends to generate samples in a narrow scope of real data space.

In all experiments, our S2M sampling adopted to cGAN-PD consistently outperforms the non-oracle baselines in terms of accuracy and diversity, *e.g.*, in CIFAR-7to3, our method improves accuracy and FID of CP-GAN by 38% and 13.74, respectively. Such improvements verify that our S2M sampling generate correct samples for joint classes, and also preserves diversity within them. Despite a large sample space of GAN, S2M sampling adopted to unconditional GAN also surpasses non-oracle baselines in terms of both fidelity and diversity while achieving reasonable accuracy. Surprisingly, despite the fact that the oracle models are trained with fully annotated data, our S2M sampling shows a comparable performance against those models using only single positive labels. Moreover, as an post-processing method, our S2M sampling fully preserves the image quality of GANs and shows the highest fidelity in terms of precision and density.

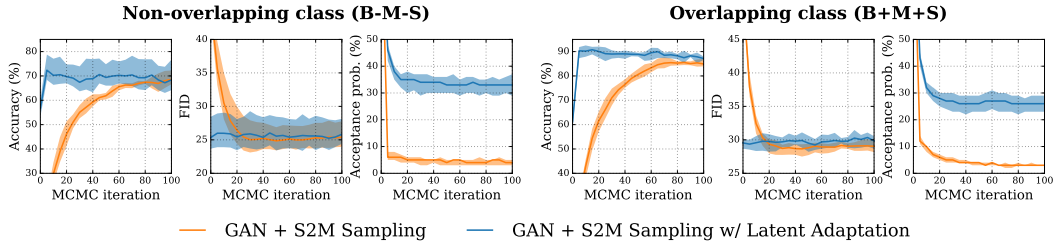

Figure 7: Accuracy (%), FID, and acceptance probability (%) per MCMC iteration for S2M sampling with and without latent adaptation.

Qualitative Results. Figure 6 depicts the results of our S2M sampling for every possible joint classes on CIFAR-7to3 and CelebA-BMS. The results show that our S2M sampling can draw diverse high-quality images from the distributions of all joint classes. Furthermore, our S2M sampling is model-agnostic and does not require the retraining of GANs. Thus, it can be easily integrated with various GANs including the state-of-the-art GANs. We depict more qualitative results of adopting our S2M sampling to unconditioanl GAN and pretrained StyleGANv2 in Appendix.

Analysis on Latent Adaptation. To demonstrate the effect of latent adaptation, we test our latent adaptation technique in a overlapping class (B+M+S) and a non-overlapping class (B-M-S) on CelebA-BMS dataset. We first perform our S2M sampling on unconditional BigGAN in these classes and draw $10k$ pilot latent samples obtained at 100 MCMC iterations. Using these latent samples, we fit Gaussian mixture of eight components as a new latent of GAN (See Appendix). Due to the discrepancy between the generator distribution and the target distribution, S2M sampling originally shows a low acceptance probability as shown in Figure 7. In this case, applying latent adaptation increases a acceptance probability and significantly improves both accuracy and FID at the early stage of iterations. This indicates that the generator distribution becomes closer to the target distribution by adopting latent adaptation, resulting in accelerating convergence speed.

5 Limitations

In general, as the number of attributes increases, the number of each joint class samples in the training dataset is drastically reduced. This may cause two main problems: (i) Training GANs to be able to generate each joint class samples becomes challenging, and our S2M sampling cannot draw samples which GANs do not generate. (ii) The computation time of the sampling procedure increases. In this case, we may need to apply latent adaptation technique to shorten MCMC chains. We provide the detailed time complexity analysis in Appendix.

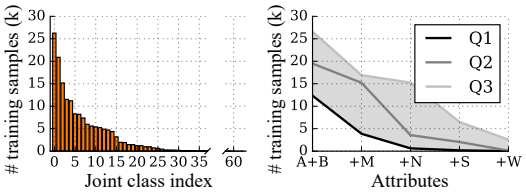

Figure 8: (Left) The distribution of the number of training samples for each joint class on CelebA-ABMNSW. (Right) As attributes are added, the quartiles of the number of samples for each joint class significantly decrease.

As shown in Figure 8, the number of training samples in joint classes rapidly decreases. Due to this nature, we use at most six attributes on CelebA dataset for experiments. Almost half of the joint classes have fewer than 100 training samples when using six attributes (*i.e.*, CelebA-ABMNSW). Nevertheless, we deal with a larger number of attributes compared to the existing methods. We believe that our work can be further extended to larger attributes with the sufficient amounts of data.

6 Conclusion

We investigate the single positive setting in the class-conditional generation task and propose a novel sampling framework called S2M sampling. We demonstrate that our proposed S2M sampling can accurately draw high quality multi-label samples in the single positive setting. To improve the sampling efficiency, we also introduce the latent adaptation technique. We believe that our theoretical framework provides a better understanding for weakly-supervised multi-label data generation. Our S2M sampling has the potential to be applied to a wide variety of generative models as well, including clustering based GANs [41] and diffusion models [42, 43], among others.

References

[1] Ian J. Goodfellow, Jean Pouget-Abadie, Mehdi Mirza, Bing Xu, David Warde-Farley, Sherjil Ozair, Aaron C. Courville, and Yoshua Bengio. Generative adversarial nets. In *Proc. the Advances in Neural Information Processing Systems (NeurIPS)*, 2014.

[2] Andrew Brock, Jeff Donahue, and Karen Simonyan. Large scale GAN training for high fidelity natural image synthesis. In *Proc. the International Conference on Learning Representations (ICLR)*, 2019.

[3] Tero Karras, Timo Aila, Samuli Laine, and Jaakko Lehtinen. Progressive growing of gans for improved quality, stability, and variation. In *Proc. the International Conference on Learning Representations (ICLR)*, 2018.

[4] Taesung Park, Ming-Yu Liu, Ting-Chun Wang, and Jun-Yan Zhu. Semantic image synthesis with spatially-adaptive normalization. In *Proc. of the IEEE conference on computer vision and pattern recognition (CVPR)*, 2019.

[5] Ming-Yu Liu, Thomas Breuel, and Jan Kautz. Unsupervised image-to-image translation networks. In *Proc. the Advances in Neural Information Processing Systems (NeurIPS)*, 2017.

[6] Jun-Yan Zhu, Taesung Park, Phillip Isola, and Alexei A. Efros. Unpaired image-to-image translation using cycle-consistent adversarial networks. In *Proc. of the IEEE international conference on computer vision (ICCV)*, 2017.

[7] Phillip Isola, Jun-Yan Zhu, Tinghui Zhou, and Alexei A. Efros. Image-to-image translation with conditional adversarial networks. In *Proc. of the IEEE conference on computer vision and pattern recognition (CVPR)*, 2017.

[8] Yunjey Choi, Min-Je Choi, Munyoung Kim, Jung-Woo Ha, Sunghun Kim, and Jaegul Choo. Stargan: Unified generative adversarial networks for multi-domain image-to-image translation. In *Proc. of the IEEE conference on computer vision and pattern recognition (CVPR)*, 2018.

[9] Abhinav Shrivastava, Abhinav Gupta, and Ross B. Girshick. Training region-based object detectors with online hard example mining. In *Proc. of the IEEE conference on computer vision and pattern recognition (CVPR)*, 2016.

[10] Christopher Bowles, Liang Chen, Ricardo Guerrero, Paul Bentley, Roger N. Gunn, Alexander Hammers, David Alexander Dickie, Maria del C. Valdés Hernández, Joanna M. Wardlaw, and Daniel Rueckert. GAN augmentation: Augmenting training data using generative adversarial networks. *CoRR*, abs/1810.10863, 2018.

[11] Mehdi Mirza and Simon Osindero. Conditional generative adversarial nets. *CoRR*, abs/1411.1784, 2014.

[12] Augustus Odena, Christopher Olah, and Jonathon Shlens. Conditional image synthesis with auxiliary classifier gans. In *Proc. the International Conference on Machine Learning (ICML)*, 2017.

[13] Yu-Jing Lin, Po-Wei Wu, Che-Han Chang, Edward Y. Chang, and Shih-Wei Liao. Relgan: Multi-domain image-to-image translation via relative attributes. In *Proc. of the IEEE international conference on computer vision (ICCV)*, 2019.

[14] Tsung-Yi Lin, Michael Maire, Serge J. Belongie, James Hays, Pietro Perona, Deva Ramanan, Piotr Dollár, and C. Lawrence Zitnick. Microsoft COCO: common objects in context. In *Proc. of the European Conference on Computer Vision (ECCV)*, 2014.

[15] Agrim Gupta, Piotr Dollár, and Ross B. Girshick. LVIS: A dataset for large vocabulary instance segmentation. In *Proc. of the IEEE conference on computer vision and pattern recognition (CVPR)*, 2019.

[16] Elijah Cole, Oisin Mac Aodha, Titouan Lorieul, Pietro Perona, Dan Morris, and Nebojsa Jojic. Multi-label learning from single positive labels. In *Proc. of the IEEE conference on computer vision and pattern recognition (CVPR)*, 2021.

[17] Ming Hou, Brahim Chaib-draa, Chao Li, and Qibin Zhao. Generative adversarial positive-unlabelled learning. In *Proc. the International Joint Conference on Artificial Intelligence (IJCAI)*, 2018.

[18] Siddarth Asokan and Chandra Sekhar Seelamantula. Teaching a GAN what not to learn. In *Proc. the Advances in Neural Information Processing Systems (NeurIPS)*, 2020.

[19] Takuhiro Kaneko, Yoshitaka Ushiku, and Tatsuya Harada. Class-distinct and class-mutual image generation with gans. In *Proc. of the British Machine Vision Conference (BMVC)*, 2019.

[20] Samaneh Azadi, Catherine Olsson, Trevor Darrell, Ian J. Goodfellow, and Augustus Odena. Discriminator rejection sampling. In *Proc. the International Conference on Learning Representations (ICLR)*, 2019.

[21] Ryan D. Turner, Jane Hung, Eric Frank, Yunus Saatchi, and Jason Yosinski. Metropolis-hastings generative adversarial networks. In *Proc. the International Conference on Machine Learning (ICML)*, 2019.

[22] Mingming Gong, Yanwu Xu, Chunyuan Li, Kun Zhang, and Kayhan Batmanghelich. Twin auxiliary classifiers GAN. *CoRR*, abs/1907.02690, 2019.

[23] Takeru Miyato and Masanori Koyama. cgans with projection discriminator. In *Proc. the International Conference on Learning Representations (ICLR)*, 2018.

[24] Minguk Kang and Jaesik Park. Contragan: Contrastive learning for conditional image generation. In *Proc. the Advances in Neural Information Processing Systems (NeurIPS)*, 2020.

[25] Tong Che, Ruixiang Zhang, Jascha Sohl-Dickstein, Hugo Larochelle, Liam Paull, Yuan Cao, and Yoshua Bengio. Your GAN is secretly an energy-based model and you should use discriminator driven latent sampling. In *Proc. the Advances in Neural Information Processing Systems (NeurIPS)*, 2020.

[26] Sangwoo Mo, Chiheon Kim, Sungwoong Kim, Minsu Cho, and Jinwoo Shin. Mining GOLD samples for conditional gans. In *Proc. the Advances in Neural Information Processing Systems (NeurIPS)*, 2019.

[27] Luke Tierney. Markov chains for exploring posterior distributions. *The Annals of Statistics*, 22(4):1701–1728, 1994.

[28] Yifei Wang, Yisen Wang, Jiansheng Yang, and Zhouchen Lin. Reparameterized sampling for generative adversarial networks. In *Machine Learning and Knowledge Discovery in Databases. Research Track - European Conference*, 2021.

[29] Chuan Guo, Geoff Pleiss, Yu Sun, and Kilian Q. Weinberger. On calibration of modern neural networks. In *Proc. the International Conference on Machine Learning (ICML)*, 2017.

[30] Tim Salimans, Ian J. Goodfellow, Wojciech Zaremba, Vicki Cheung, Alec Radford, and Xi Chen. Improved techniques for training gans. In *Proc. the Advances in Neural Information Processing Systems (NeurIPS)*, 2016.

[31] Martin Heusel, Hubert Ramsauer, Thomas Unterthiner, Bernhard Nessler, and Sepp Hochreiter. Gans trained by a two time-scale update rule converge to a local nash equilibrium. In Isabelle Guyon, Ulrike von Luxburg, Samy Bengio, Hanna M. Wallach, Rob Fergus, S. V. N. Vishwanathan, and Roman Garnett, editors, *Advances in Neural Information Processing Systems*, pages 6626–6637, 2017.

[32] Tuomas Kynkäänniemi, Tero Karras, Samuli Laine, Jaakko Lehtinen, and Timo Aila. Improved precision and recall metric for assessing generative models. In *Proc. the Advances in Neural Information Processing Systems (NeurIPS)*, 2019.

[33] Muhammad Ferjad Naeem, Seong Joon Oh, Youngjung Uh, Yunjey Choi, and Jaejun Yoo. Reliable fidelity and diversity metrics for generative models. In *Proc. the International Conference on Machine Learning (ICML)*, 2020.

[34] Christian Szegedy, Vincent Vanhoucke, Sergey Ioffe, Jonathon Shlens, and Zbigniew Wojna. Rethinking the inception architecture for computer vision. In *Proc. of the IEEE conference on computer vision and pattern recognition (CVPR)*, 2016.

[35] Y. Lecun, L. Bottou, Y. Bengio, and P. Haffner. Gradient-based learning applied to document recognition. *Proceedings of the IEEE*, 86(11):2278–2324, 1998.

[36] François Denis. PAC learning from positive statistical queries. In *ALT*, Lecture Notes in Computer Science, 1998.

[37] François Denis, Rémi Gilleron, and Fabien Letouzey. Learning from positive and unlabeled examples. *Theor. Comput. Sci.*, 2005.

[38] Xiang Wei, Boqing Gong, Zixia Liu, Wei Lu, and Liqiang Wang. Improving the improved training of wasserstein gans: A consistency term and its dual effect. In *Proc. the International Conference on Learning Representations (ICLR)*, 2018.

[39] Hui Chen, Fangqing Liu, Yin Wang, Liyue Zhao, and Hao Wu. A variational approach for learning from positive and unlabeled data. In *Proc. the Advances in Neural Information Processing Systems (NeurIPS)*, 2020.

[40] Florent Chiaroni, Ghazaleh Khodabandelou, Mohamed-Cherif Rahal, Nicolas Hueber, and Frédéric Dufaux. Counter-examples generation from a positive unlabeled image dataset. *Pattern Recognition*, 107:107527, 2020.

[41] Arantxa Casanova, Marlène Careil, Jakob Verbeek, Michal Drozdzal, and Adriana Romero-Soriano. Instance-conditioned GAN. In *Proc. the Advances in Neural Information Processing Systems (NeurIPS)*, 2021.

[42] Jonathan Ho, Ajay Jain, and Pieter Abbeel. Denoising diffusion probabilistic models. In *Proc. the Advances in Neural Information Processing Systems (NeurIPS)*, 2020.

[43] Prafulla Dhariwal and Alexander Quinn Nichol. Diffusion models beat gans on image synthesis. In *Proc. the Advances in Neural Information Processing Systems (NeurIPS)*, 2021.

Checklist

1. For all authors...
   (a) Do the main claims made in the abstract and introduction accurately reflect the paper's contributions and scope? [Yes]
   (b) Did you describe the limitations of your work? [Yes] See Section 5.
   (c) Did you discuss any potential negative societal impacts of your work? [Yes] See Appendix.
   (d) Have you read the ethics review guidelines and ensured that your paper conforms to them? [Yes]
2. If you are including theoretical results...
   (a) Did you state the full set of assumptions of all theoretical results? [Yes]
   (b) Did you include complete proofs of all theoretical results? [Yes] See Appendix.
3. If you ran experiments...
   (a) Did you include the code, data, and instructions needed to reproduce the main experimental results (either in the supplemental material or as a URL)? [Yes] We provide the codes in the supplemental material.
   (b) Did you specify all the training details (e.g., data splits, hyperparameters, how they were chosen)? [Yes] See Appendix.
   (c) Did you report error bars (e.g., with respect to the random seed after running experiments multiple times)? [Yes] We reported the standard deviation in the experimental results.

(d) Did you include the total amount of compute and the type of resources used (e.g., type of GPUs, internal cluster, or cloud provider)? [Yes] See Appendix.

4. If you are using existing assets (e.g., code, data, models) or curating/releasing new assets...
   (a) If your work uses existing assets, did you cite the creators? [Yes]
   (b) Did you mention the license of the assets? [No] We used publicly available benchmark datasets: MNIST, FMNIST, CIFAR10, CelebA, and CelebA-HQ.
   (c) Did you include any new assets either in the supplemental material or as a URL? [Yes] We provide the codes in the supplemental material.
   (d) Did you discuss whether and how consent was obtained from people whose data you're using/curating? [Yes] The benchmark datasets used in our paper are widely used for research purpose.
   (e) Did you discuss whether the data you are using/curating contains personally identifiable information or offensive content? [Yes] The benchmark datasets used in our paper are widely used by others and do not contain any offensive contents.

5. If you used crowdsourcing or conducted research with human subjects...
   (a) Did you include the full text of instructions given to participants and screenshots, if applicable? [N/A]
   (b) Did you describe any potential participant risks, with links to Institutional Review Board (IRB) approvals, if applicable? [N/A]
   (c) Did you include the estimated hourly wage paid to participants and the total amount spent on participant compensation? [N/A]